J12.3 PHOENIX URBAN HEAT ISLAND EXPERIMENT: EFFECTS OF BUILT ELEMENTS

S. Di Sabatino[1,2,*], B. C. Hedquist[1,3], W. Carter[1], L. S. Leo[2], H. J. S. Fernando[1]
[1]Environmental Fluid Dynamics Program, ASU, Tempe, AZ, USA
[2]Dipartimento di Scienza dei Materiali, Università del Salento, Lecce, Italy
[3]School of Geographical Sciences, ASU, Tempe, AZ, USA

1. INTRODUCTION

Rapid growth of the urbanization process, which is occurring worldwide (UN, 2007), is one of the biggest issues that society has to face in future years. This is because of the associated increase of energy and water consumption, climatic impacts, human health and comfort. The development of the so called urban heat island (UHI) (Oke, 1982, 1987) is one of the most evident phenomena associated with urban settlements. The urban heat island can be simply defined as the temperature difference ΔT_{u-r} between the urban area and its surrounding rural environment. In general terms, the UHI is becoming more intense as city sizes increase and most importantly, it greatly contributes to exacerbating those issues outlined above (Changnon *et al*., 1996, Rosenfeld *et al*., 1998, Konopacki and Akbari, 2002, Rizwan *et al*., 2007).

In hot environments, such as in large cities in the sub(tropics), where the size of the cities is growing the fastest (UN, 2007), the impact of UHI can be serious. In those cities, very often, no relief from heat is experienced during summer nights with consequences on a person's well-being, thus becoming a serious threat for human health. In addition, measures adopted to try to mitigate UHI might have a great impact on city economics. This might be very onerous especially for cities located in developing countries and/or in less fortunate places of the world. These cities often suffer from a lack of infrastructures and adequate measures to face global environmental changes. Even though this might not be the case for the city of Phoenix, Arizona, it is evident that this region of the US southwest has undergone rapid change in the last fifty-sixty years. The city has recorded a rapid enlargement and large portion of the land and desert vegetation have been replaced by buildings, asphalt and concrete (Brazel *et al*., 2007, Emmanuel and Fernando, 2007). Measurements in Phoenix area have shown that minimum air temperature is increasing fast. Besides, model predictions show that minimum air temperatures for Phoenix metropolitan area in future years might be even higher than 38 °C in the near future. Motivated by this experimental evidence and by the interest for the development of UHI mitigation strategies in hot and arid environments, a one-day intensive experiment was conducted on the 4th-5th April 2008 in Phoenix. Inter alia, infrared thermography (IRT) was used for UHI mapping. The experiment had a series of ambitious objectives: 1) to measure a complete diurnal cycle of surface and air temperature throughout the Phoenix metropolitan area. This was done in order to quantify UHI at various scales, namely the city scale, the neighborhood scale down to the street canyon, and building scale; 2) to highlight possible flow modifications induced by the city by extra thermal forcing; 3) to derive a general methodology for addressing physical processes at the basis of UHI formation; 4) to suggest mitigation strategies for dealing with UHI in the Phoenix area and in more general terms; 5) to identify input parameters for numerical mesoscale models and give suggestions for heat parameterizations in those models.

2. BACKGROUND

For many years, scientists addressing UHI have focused their attention on specific aspects but a comprehensive knowledge of how to efficiently investigate and to deal with UHI is still missing. As outlined by some authors, despite the abundance of UHI studies (see for instance Arnfield, 2003 for a review), little attention has been given to investigate relations between single observations and the large number of physical-chemical processes occurring within the urban atmospheric layer. Many UHI studies focus on field observations using various instrumentations. Experimental conditions refer to a relatively large volume of air containing significant spatial and temporal variability. Further complications arise from the inherent complexity of the urban morphological structure, complicated flow patterns, energy sources/sinks, and so on.

Physical-mathematical modeling has become the most important tool overall in the last few decades, although the suitability of process-response models is limited by the extent to which the physics of the processes are understood. Some progress has been made in this direction. The effect of buildings on flow and temperature fields within the urban canopy layer is being addressed in later years (e.g. Belcher *et al*., 2003). Several urban flow and energy parameterizations are also available. However, there are fewer studies addressing the thermal aspects of the urban environment and the spatial temperature distribution within urban street canyons. Due to flow separation from buildings and the consequent asymmetric pressure field around them, the exchange of momentum in the urban environment is more efficient than the exchange of scalar quantities, such as temperature or moisture. Due to the very high mechanical forcing induced by the buildings, attention to flow modifications induced hot surfaces in real conditions have only rarely been addressed (Solazzo and Britter, 2007). In the later, it has been outlined that in most real scenarios buoyancy effects are confined near the wall and therefore a little contribution to the overall flow structure is to be expected.

Results derived from data collected during the Phoenix UHI experiment provide a good opportunity for

investigating several aspects following the objectives outlined in the previous section. Even though work is ongoing, in this paper we focus on the effect of heated individual buildings on temperature patterns measured in the inner core of the city. In this respect, the choice of the scale, being that of the building and street canyon scale. At this point we do not investigate impacts on the other scales but we will infer some of the implications.

3. METHODOLOGY

3.1 *Description of downtown measurements*

The general setup of the experiment and details of the overall instrumentation employed is given in a companion paper (Hedquist *et al*., 2009). Here we only report on details of the infrared images taken in the Central Business District (CBD). This area is characterized by the presence of several high-rise buildings, some of them being more than 100 m tall. Building façades have a wide range of materials ranging from concrete to glass, often being present in combination to form a grid-like structure in most cases.

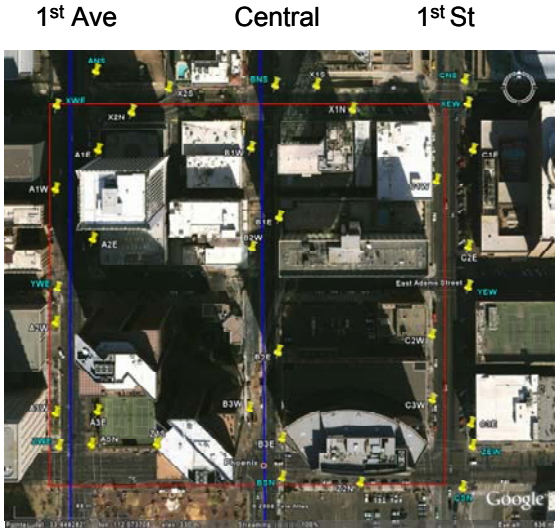

Figure 1: Sketch of the study area in downtown Phoenix adapted from Google Earth. The red line encompasses the area investigated using a hand-held IR camera. Yellow marks show measurement positions.

Buildings and measurement locations are shown in Figure 1. In total, about two thousand images using a FLIR IR thermal camera (FLIR, 2008) were taken during the 24-hour campaign. Images were taken at regular intervals of two hours throughout the day starting from 0600 LST. This was possible using an hand-held IR camera operating while being transported on a special bicycle platform ("pedicab" or bicycle taxi). This special equipment allowed us to move quickly through normal working day traffic from one location to the other. About twenty building façades and several street canyons were surveyed during each measurement interval. Images were taken using a standard camera set-up. The distance was set at 100 m, with an average between 50 and 200 m corresponding to the distance between the object and the camera position. Maximum distance was limited by the street canyon width where images were taken. To be able to maintain a similar resolution for all images, several shots of portions of the same building façade at several heights were taken. Those images were then assembled in one single infrared image using FLIR ThermaCam Image Builder Software. The use of ThermaCAM™ Researcher Software allowed us to perform a preliminary analysis of the overall images as well as an in-depth analysis of mean radiant temperature. A sensitivity analysis was carried out to verify camera settings which were maintained the same during the all experiment. The most important object parameter is its emissivity because it is a measure of how much radiation is emitted from an object in comparison with that from a perfect blackbody at the same temperature. During the measurement campaign we set an emissivity value of 0.96. Sensitivity analysis confirmed that it was appropriate for material such as concrete and dark glass, due to these materials being the main constituents of CBD buildings facades. Results of the analysis are presented and discussed in the next section.

3.2 *CFD modelling set-up*

To complete the analysis a general numerical Computational Fluid Dynamics (CFD) model was employed. Simulations were used to aid measurement interpretation. In particular, we were interested in possible flow modifications induced by temperature surface gradients which were not directly measured during the experiment as well as identifying temperature distribution within the canyons.

CFD simulations were carried out by considering an approaching boundary layer flow. Reynolds averaged equations with a standard k-ε turbulence closure (Launder and Spalding, 1974) together with the Fourier equation were considered for flow and temperature, respectively. The Boussinesq approximation was assumed.

Wind speed U, specified as an inlet boundary condition, was assumed to follow a logarithmic profile:

$$U = \frac{u_*}{\kappa}\ln\left(\frac{z+z_0}{z_0}\right)$$

where u_*=0.25 m/s is the friction velocity, κ the von Kàrmàn constant (0.40) and z_0=0.4 m the roughness height. Turbulent kinetic energy and dissipation rate profiles were specified as follows:

$$k = \frac{u_*^2}{\sqrt{C_\mu}}\left(1-\frac{z}{\delta}\right) \quad \& \quad \varepsilon = \frac{u_*^3}{\kappa z}\left(1-\frac{z}{\delta}\right)$$

where δ is the boundary layer depth and C_μ=0.09. Symmetry boundary conditions were specified on the top and lateral sides of the computational domain. A termination criterion of 10^{-5} was used for all field variables. Several computations were made using both

a simplified geometry of individual buildings shown in Figure 1 and one street canyon. The computational domain used for flow simulations without heated walls was a parallelepiped with dimensions of 2625 m (in the x direction, parallel to the flow direction) by 854 m (in the y direction) by 620 m (vertical z direction). This simulation was used to obtain some qualitative information about flow patterns in the area investigated. The effect of temperature for this geometry is left to future investigations. Figure 2 shows results of the simulation.

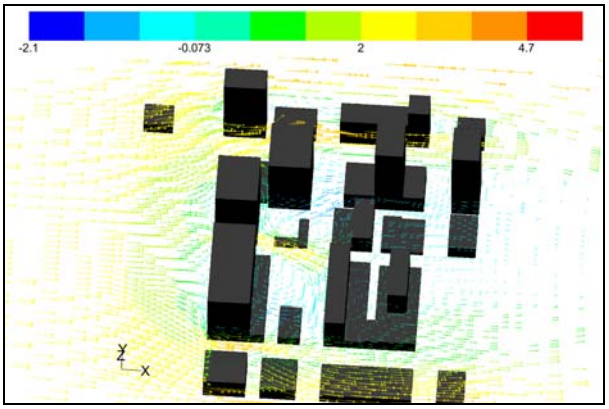

Figure 2. Flow patterns at z= 30 m without temperature forcing for Phoenix downtown using a simplified geometry.

Figure 2 illustrates the complex flow patterns which developed within buildings, where vortices behind tall buildings, flow separations and accelerated flow at the building top and along the canyons are present. For example, a two canyon-vortex structure is visible between the tallest buildings characterized by high turbulence affecting among others diffusion of heat and other scalars. As we were mainly interested on flow modifications occurring at the street canyon and building scale, a single street canyon was chosen for detailed numerical investigations. In particular, we chose the street canyon of 1st Avenue as temperature measurements were available for almost all buildings forming the canyon. A similar choice was made by Hedquist *et al*. (2008) in their numerical simulations using ENVI-met (ENVI-met, 2008).

Figure 3 shows the street canyon geometry used in the CFD simulations. Building shapes are partially simplified with respect to the real ones, but we maintained same building heights and relative distances between buildings as in the reality. The total area enclosed by the buildings is 128 m by 254 m.

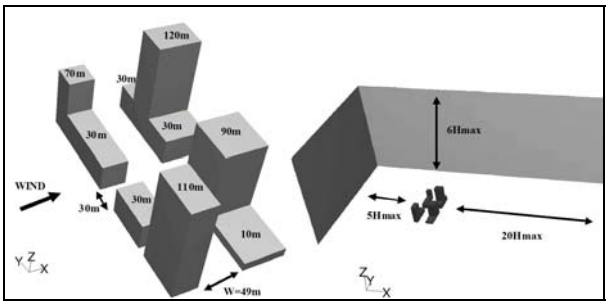

Figure 3: Sketch of the street canyon geometry (left graph) with the height of each building indicated on the roof and details of the computational domain (right graph) used for street canyon CFD simulations.

Overall the street canyon is asymmetric as buildings at both sides do not have the same height. The heights of buildings range from 10 m to Hmax=120 m, while the width W is equal to 49 m. The "average" height of buildings at both sides is about 60 m leading to an aspect ratio W/H equal to about 1.2. However, it is clear that the flow which developed inside the canyon was strongly affected by the relative heights of each individual building. Moreover, an intersection is also present in the geometry affecting the flow substantially.

The computational domain was built using hexahedral elements (about an overall of two millions cells) with a finer resolution in the volume occupied by the buildings, where the smallest dimensions of the elements were $\delta x_{min}=\delta y_{min}=3$m and $\delta z_{min}=0.5$m. Outside, the expansion rate between two consecutive cells was below 1.3. Several tests were performed to verify grid size independence. The distance from the inlet plane to the first building of the street canyon was 5Hmax, the distance from the top of the domain to the ground was 6Hmax and the distance from the outflow plane to the downstream building was 20Hmax. This was done following suggestions from the relevant CFD literature for similar problems (see for instance Di Sabatino *et al*., 2007).

4. RESULTS

4.1 *Analysis of building thermography measurements*

Figure 4 is a schematic representation of the building layout within the study area. In particular, the figure shows labels used to identify those buildings that we have surveyed. Colors qualitatively indicate building having similar maximum temperature. As we are mainly interested in studying temperature distribution within the air layer most crucial for outdoor human comfort, these values, extracted from thermal IR images, represent surface building temperatures close to the ground.

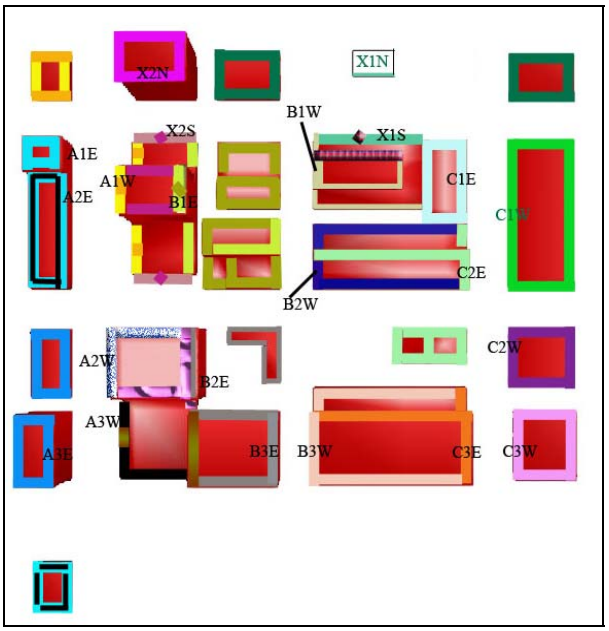

Figure 4: Building layout of the study area and with colors indicating qualitative temperature of buildings with the same temperature.

Based on the analysis of infrared images, Figure 5 resumes the main features of warming/cooling diurnal cycle experienced by the façades in the Phoenix CBD. The figure shows the diurnal variation of the mean radiant temperature for six buildings, each of which is representative of a different portion of the study area. The mean radiant temperature is the average of all temperature readings on the entire building façade. In particular, we consider two buildings for each of the three street canyons oriented along the North-South direction. These are denominated as canyons A, B and C. Buildings denoted with E are those facing East and representative of West side of the canyon while those denoted with W have facades facing West and therefore they are representative of East side of the canyon. Looking at the top graph of Figure 5, it is evident that the North-South canyon orientation results in a maximum mean radiant temperature of about 34 °C on west walls about 2 hours before the solar noon. However, some exceptions exist, such as the C3E building which experiences a maximum of 40 °C at nearly 8:00 am. This is probably because Eastern high buildings shadowing the façades are absent in front of C3E; instead shadowing buildings are present in front of A3E and B3E (see Fig. 4). Analogous considerations can be made for the East side of canyon but now the temperature peak is shifted about 2 hours after noon, with the exception of the A1W façade. In fact, A1W is higher than the building in front of it while the situation is reversed for B3W and C3W façades. Some insight on environmental conditions being affected by these hot surfaces throughout the day can be inferred by comparing those with air temperature. Figure 5 shows air temperatures both measured in-situ at about 2 m and at Phoenix Sky Harbor Airport at 10 m height. Analysis of these curves suggests: 1) an abrupt excursion experienced by building façades during the day; 2) a maximum air temperature difference between two sites of about 7 °C during the day around 1pm and about 6 °C after 11pm. This air temperature difference is maintained almost throughout the night. Furthermore, it appears that air temperature profile correlates roughly with surface temperature of buildings facing the West. Air temperature rise within the CBD is accompanied by a rapid cooling of building façades, suggesting warm air previously heated being transported from adjacent areas.

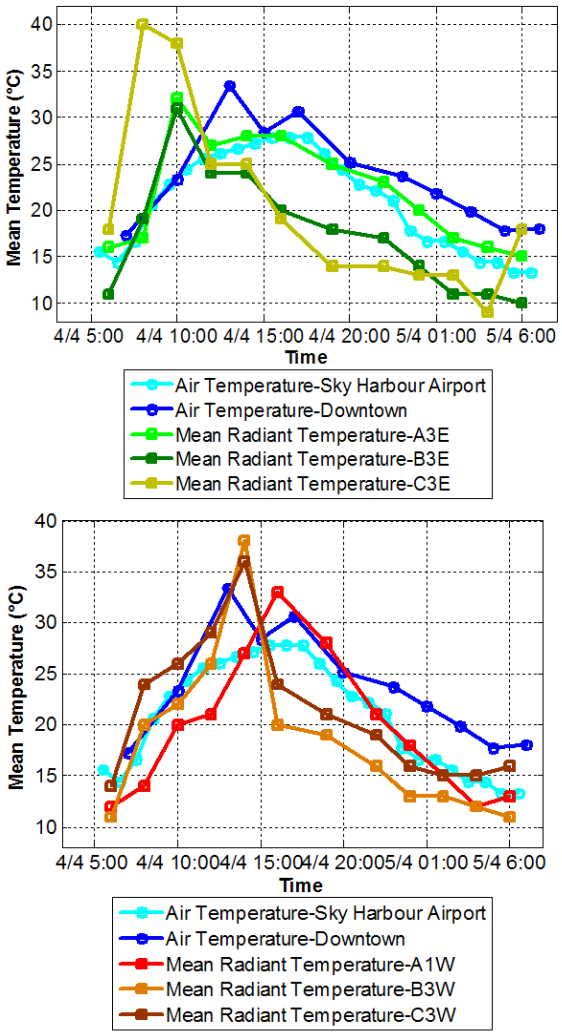

Figure 5: Comparison of diurnal mean radiant temperatures related to different western (top) and eastern (bottom) building façades. Profiles of air temperature are also reported.

Figure 6 shows as an example of diurnal mean radiant temperatures related to different portions of the building façade for both a western (top) and an eastern (bottom) building. It can be observed that the cooling/warming processes of building façades are not homogeneous showing a specific dependence with elevation and building exposure. In particular, the A3E

façade shows an intense temperature peak at the building bottom which decreases linearly with elevation. The A1W façade shows a different behavior with the bottom and highest façade portions being warmer through the day than the middle portion. In order to emphasize the role played by the different materials in determining overall façade mean temperature, profiles of temperature corresponding to dark glass and concrete have been reported in Figure 7. These curves suggest the major contribution to heat storage due to concrete material which remains nearly the same temperature throughout day.

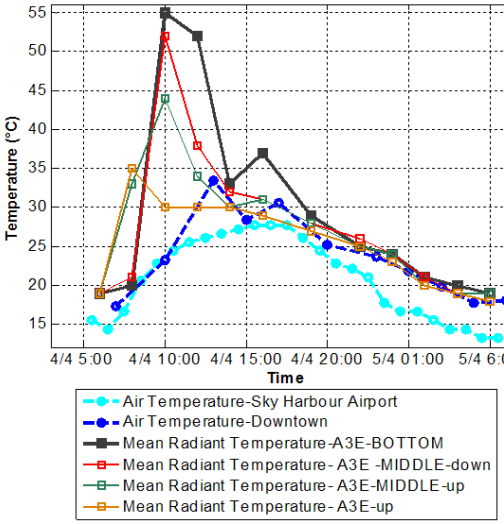

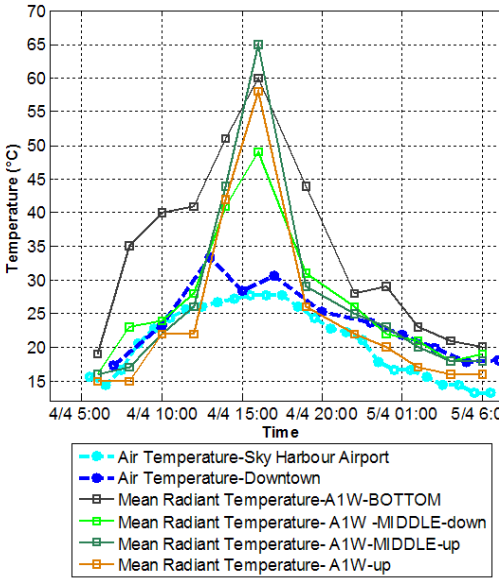

Figure 6: Comparison of diurnal mean radiant temperatures related to different portion of the façade for both a western (up) and an eastern (bottom) building. Profiles of air temperature are also reported.

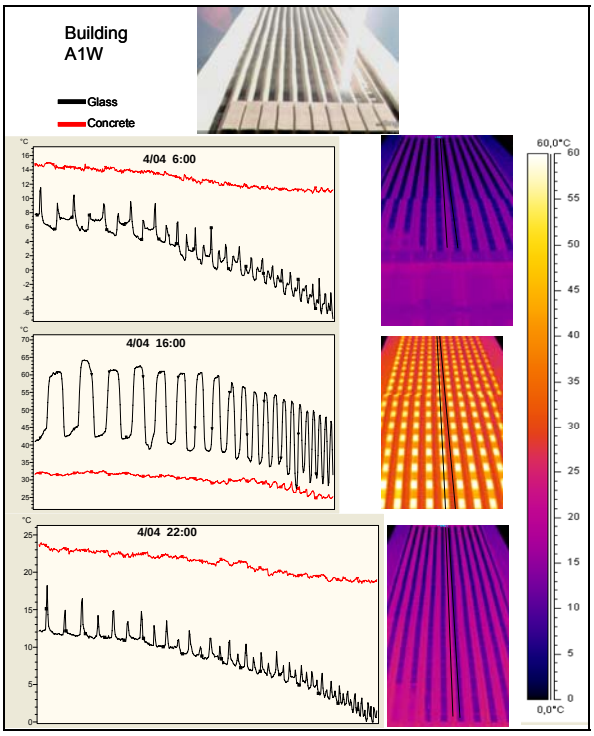

Figure 7: Comparison of mean radiant temperatures related to dark glass and concrete constituting the façade of the A1W building.

4.2 *Analysis of CFD simulations*

Buoyancy effects are studied by means of the dimensionless Richardson number defined as:

$$Ri = \frac{[g(T_w - T_a)L]}{T_a u_H^{\,2}}$$

where g is the gravitational acceleration, T_w is the wall temperature, T_a=15 °C is the ambient air temperature, L is a characteristic length, and u_H is a reference velocity set at the building height in the incoming flow. We also fixed the same temperature of the air for building walls and roofs (15 °C) except for the leeward and windward side. Different cases with and without heating at ground level, leeward and windward sides of the street canyon are analyzed (see Table 1). Temperatures are those measured at 10pm.

Case	T_{ground} (°C)	$T_{leeward/windward}$ (°C)
1 (reference case)	NO HEAT	
2	20 (measured temperature)	Measured temperatures (gradient)
3	23 (average of all temperature measurements)	
4	20 (measured temperature)	Average temperature for each building

Table 1. Simulations of wall heating in the street canyon.

In particular, we simulated four cases. Case1 is the isothermal reference case with no extra wall heating being specified. Case2 and Case4 are characterized both by the same temperature at the ground. They differ from each other only because of building wall temperature. This is constant in Case4 while an average temperature profile derived from infrared images of individual building facades forming the street canyon was imposed in Case2. Case3 has the same average temperature for the ground, the leeward and the windward sides of all buildings.

Figure 8 shows, as an example, vectors of the wind velocity at several planes for the reference case. In particular, the horizontal planes refer to z=30m and z=70m. The vertical plane y=50m cuts the portion of the canyon characterized by H=30m at both sides. The vertical plane y=-110m cuts the portion of the canyon characterized by H=110m at the leeward and H=10m at the windward (Figure 3).

The analysis of simulation results for cases with wall heated (not shown here) reveals a weak flow dependence of the heating within the canyon. In fact, overall the qualitative behavior of the flow is similar in every case considered. This implies that, for the considered canyon geometry and boundary conditions, heating differently leeward, windward and ground do not affect greatly the general flow patterns. Probably the particular geometry of the street canyon, which is quite wide, makes the buoyancy effect not significant enough with respect to the mechanical one which, in turn, is the dominant effect.

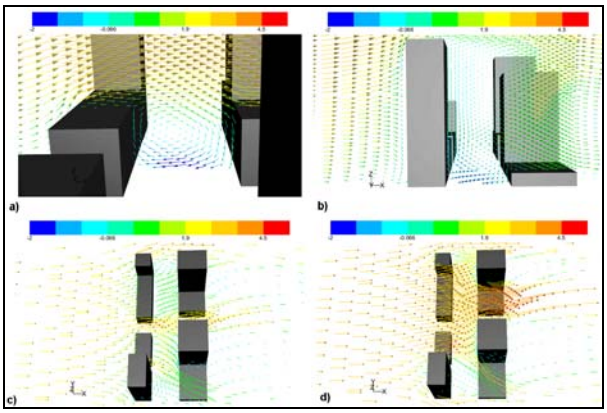

Figure 8: Vectors of x-velocity at y=50m (a), y=-110m (b), z=30m (c) and z=70m (d).

From horizontal and vertical z-velocity profiles shown in Figure 9, it is possible to appreciate a low effect of buoyancy both in the center and at sides of the whole street canyon. Vertical profiles refer to the last portions of the canyon at both sides (see Figure 3). In particular, we note that near the ground, the buoyancy effect is significant in the vicinity of the middle of the intersection, while above the effect is visible at sides of the canyon. This is due to stagnant conditions behind tall buildings which enhance the effect of buoyancy with respect to the mechanical ones. Figure 9 also shows that no significant flow modifications are visible at the street canyon scale due to different wall heating (Case2, 3 and 4). However, flow patterns within the canyons result to be more sensitive when a wall temperature gradient (the one corresponding to temperature measurements) is imposed (Case2).

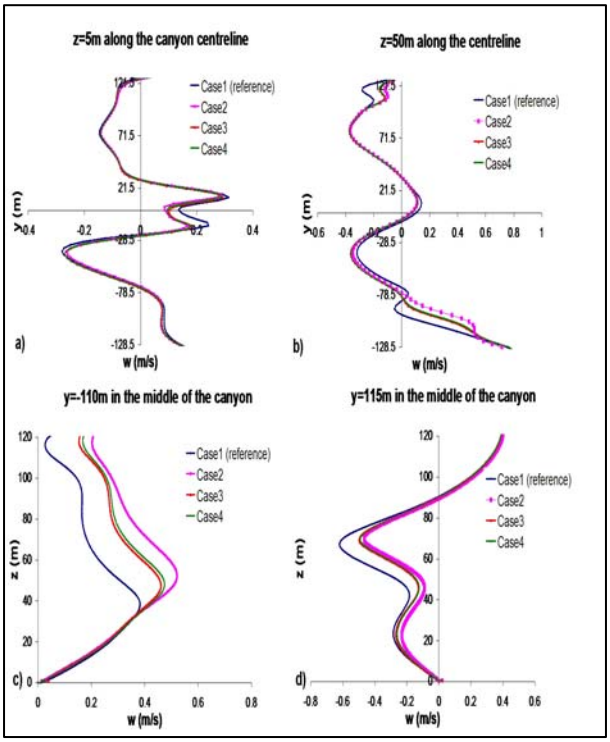

Figure 9: Vertical z-velocity profiles at z=5m (a), z=-50m (b), y=115m (c) and y=-110m (d).

Overall, results showed that flow and turbulence developed within the canyon produced a temperature distribution spatially uniform (apart from a relatively thin near-wall thermal boundary layer), as already found by Solazzo and Britter (2007). Moreover, we should note that the maximum difference in temperature between air and wall is about 14 °C and that the undisturbed velocity at 10 m is 2 m/s. In these conditions, we would expect a significant influence of buoyancy at least in those portions of the canyon characterized by stagnant conditions and large temperature differences. However, probably the air approaching the canyon had been already heated and consequently its temperature was not so different from that imposed at walls.

5. CONCLUSIONS

The Phoenix UHI experiment has allowed us to gain detailed knowledge about surface temperature within the Phoenix CBD area. The use of Thermal IR images have allowed for careful investigations of temperature distributions at a fine resolution. Building façade temperature recorded through a complete diurnal cycle has shown that through the day can be very high with an average of 40 °C. During the night, air temperature correlates well with surface temperature.

Analysis suggests how most of the heat is trapped in the inner core of the street canyon with temperature being maintained constant within a layer about 30 m deep. This has been confirmed by CFD investigations. Vortices formations between tall buildings and the complex flow structure generated by high-rise buildings dominate flow dynamics. Thermal forcing only weakly affects flow fields. A small flow modification has been observed due to wall temperature gradients during the night. Results suggest to the overall flow modifications is occurring at a larger scale.

Work is ongoing to further analyse implications of the measurements. We plan to further investigate in more details the effect of buoyancy on flow inside the canyon and within the whole study area. A sensitivity test will be that of improving the modelling set-up of the problem in order to assure the CFD code to conserve the imposed temperatures at walls as boundary conditions.

6. ACKNOWLEDGEMENTS

The authors acknowledge the kind help and support from all colleagues, students and other people who have generously contributed in various ways to the successful realization of the Phoenix Urban Heat Island experiment. SDS acknowledges funds from the EFD Lab during her stay at ASU. The authors are very grateful to Dr. M. Brown for providing information on building height in central Phoenix and R. Buccolieri for his help in the CFD simulations.

REFERENCES

Arnfield, AJ. 2003: Two decades of urban climate research: a review of turbulence, exchanges of energy and water, and the urban heat island. *International Journal of Climatology* 23, 1-26.

Belcher, SE, Jerram, N. and Hunt, JCR, 2003: Adjustment of a turbulent boundary layer to a canopy of roughness elements. *J. Fluid Mech.* 488, 369-398.

Brazel, AJ, Gober, P., Lee, S., Grossman-Clarke, S., Zehnder, J., Hedquist, B. and Comparri, E 2007: Dynamics and determinants of urban heat island change (1990-2004) with Phoenix, Arizona, USA. *Climate Research* 33, 171-182.

Changnon, SA, Kunkel, KE and Reinke, BC 1996: Impacts and Responses to the 1995 heat wave: a call to action. *Bullettin of the American Meteorological Society* 77, 1497-1505.

Di Sabatino, S., Buccolieri, R., Pulvirenti, B. and Britter, RE 2007: Simulations of pollutant dispersion within idealised urban-type geometries using CFD and integral models. *Atmospheric Environment* 41, 8316-8329.

Emmanuel, R. and Fernando HJS 2007: Effects of urban form and thermal properties in urban heat island mitigation in hot humid and hot arid climates: The cases of Colombo, Sri Lanka and Phoenix, USA. *Climate Research* 34, 241-251.

ENVI-met 2008: ENVI-met software home page. http://www.envi-met.com.

Fluent, 2008: User's Manual. http://www.fluent.com.

FLIR 2008: *History of Infrared Technology and Thermal Imagers*. http://www.flirthermography.com. Accessed July 31, 2008.

Hedquist, BC, Brazel, AJ, Di Sabatino, S., Carter, W. and Fernando, HJS 2009: Phoenix urban heat island experiment: micrometeorological aspects. *Proceedings of the Eighth Symposium on the Urban Environment,* Phoenix, Arizona.

Konopacki, S., and Akbari, H. 2002: Energy Savings of Heat-Island Reduction Strateegies in Chicago and Houston, Lawrence Berkeley National Laboratory Report LBNL-49638, Berkeley, CA, 2002.

Launder, BE and Spalding, DB 1974: The Numerical Computation of Turbulent Flows. *Computer Methods in Applied Mechanics and Engineering* 3, 269-289.

Oke, TR 1982: The energetic basis of the urban heat island. *Quarterly Journal of the Royal Meteorological Society* 108, 1-24.

Oke, TR 1987: *Boundary Layer Climates*. 2nd ed. Methuen. 435 pp.

Rizwan, AM, Dennis, YCL, Liu, C. 2008: A review on the generation, determination and mitigation of Urban Heat Island. *Journal of Environmental Sciences* 20, 120–128

Rosenfeld, AH, Akbari, H. and Romm, JJ, 1998: Cool communities: Strategies for heat island mitigation and smog reduction. *Energy and Buildings* 28**,** 51–62.

Solazzo, E. and Britter, R. 2007: Transfer processes in a simulated urban street canyon. *Boundary-Layer Meteorology* 124, pp. 43–60.

United Nations, Department of Economic and Social Affairs, Population Division, 2007. *World Population Prospectus: The 2006 Revision*. Highlights, Working Paper No. ESA/P/202.2.